Int. J. Microgravity Sci. Appl., **34** (4) (2017) 340405
DOI: 10.15011//jasma.34.340405

IIIII AMS2016 Proceedings 2 IIIII
(Original Paper)

Acceleration of the Macroscopic Contact Line of a Droplet Spreading on a Substrate after Interaction with a Particle

Daichi KONDO[1], Lizhong MU[2,3], Frédérick de MIOLLIS[4], Tetsuya OGAWA[5], Motochika INOUE[1], Toshihiro KANEKO[2,5], Takahiro TSUKAHARA[2,5], Harunori N. YOSHIKAWA[6], Farzam ZOUESHTIAGH[4] and Ichiro UENO[2,5]

Abstract

We focus on dynamic behavior of the macroscopic contact line (MCL) of a droplet spreading on a substrate after an interaction with a spherical particle settled on the substrate. We will show that there exist three different regimes of the MCL behavior for different ranges of the capillary number. In the case of a small capillary number, the MCL exhibits a sharp acceleration after the interaction with the particle that remains at its original position In the case of a large capillary number, on the other hand, the MCL advances without any significant variation of behavior produced by the interaction with the particle. The particle is sucked toward the bulk of the droplet after the interaction. In the case of a moderate capillary number, the MCL exhibits gradual acceleration after the interaction with the particle, accompanied by a slight movement of the particle toward the droplet. We will also discuss the effect of the particle size on the behaviors of the MCL.

Keywords: macroscopic contact line (MCL), dynamic wetting, spherical particle, environmental control.
Received: 2 January 2017, Accepted 28 September 2017, Published 31 October 2017

1. Introduction

Wetting of solid surfaces is a ubiquitous natural phenomenon. When a liquid droplet is placed at a solid surface, the droplet exhibits either complete or partial wetting. These two regimes are distinguished by the spreading parameter S, which is related to the surface tension[1)]. The spreading of a droplet on a solid substrate is accompanied by the movement of the macroscopic contact line (MCL), which is the visible boundary line of the solid-liquid-gas interface[2)]. In order to predict and control the behavior of the liquid on a solid surface, it is necessary to consider the spreading of the liquid in industrial applications such as cleaning, cooling, coating, and microchannel devices. In particular, comprehensive understandings of the dynamics and the control of the behavior of the wetting are necessary for transporting liquid under microgravity. The wetting phenomenon has been widely studied for over 200 years; including research by Young[3)] and Laplace[4)]. For a non-volatile liquid droplet spreading on a solid surface, the capillary number ($\mathrm{Ca} = \mu V_{CL}/\gamma$) and Weber number ($\mathrm{We} = \rho V_{CL}^2 L/\gamma$) are the key parameters that characterize the spreading on the macroscale[5, 6)], where μ and ρ are the dynamic viscosity and density of the liquid, respectively, V_{CL} is the MCL velocity, γ is the surface tension, and L is the characteristic length. Hoffman[5)] experimentally studied the wetting phenomenon by pushing a liquid in a thin tube and thereby developed the correlation between the dynamical contact angle and the capillary number; it was found that the capillary force becomes dominant under $\mathrm{Ca} \leq 10^{-5}$. Lopez et al.[7)] focused on the late stage of the spreading of a liquid droplet on a smooth substrate, under which the gravity and fluid viscosity became dominant. They proposed a theoretical model to indicate the radius of the spreading droplet proportional to $t^{1/8}$, where t is the spreading time. Tanner[8)] developed the dynamical relations of the spreading radius and the contact angle using a smooth substrate and a non-volatile liquid through the experimental approach. In the

1. Division of Mechanical Engineering, Graduate School of Science and Technology, Tokyo University of Science, 2641 Yamazaki, Noda, Chiba 278-8510, Japan.
2. Research Institute for Science and Technology (RIST), Tokyo University of Science, 2641 Yamazaki, Noda, Chiba 278-8510, Japan.
3. Key laboratory of Ocean Energy Utilization and Energy Conservation of Ministry of Education, School of Energy and Power Engineering, Dalian University of Technology, No.2 Linggong Road, Ganjingzi District, Dalian City, Liaoning Province 116024, China.
4. Univ. Lille, CNRS, ECLille, ISEN, Univ. Valenciennes, UMR 8520 - IEMN, F-59000 Lille, France.
5. Department of Mechanical Engineering, Faculty of Science and Technology, Tokyo University of Science, 2641 Yamazaki, Noda, Chiba 278-8510, Japan.
6. Université Côte d'Azur, CNRS, UMR 7351, Laboratoire J.-A. Dieudonné, 06108 Nice Cedex 02, France.
(E-mail: ich@rs.tus.ac.jp)

case of capillary-dominant stage, it was indicated that the radius of the spreading droplet is proportional to $t^{1/10}$. Then, Cazabat and Cohen Stuart[9] conducted a series of experiments on the droplet spreading on a smooth substrate, and clearly indicated the transition from capillary-dominant stage[8] to gravity-viscosity-dominant stage[7].

Kralchevsky and Nagayama[10, 11] studied the interaction between particles and liquid, particularly focusing on correlation between the contact angle and the surface tension. Ally et al.[12] measured the force on a single spherical particle in interaction with a liquid film when the particle approached to and subsequently retracted from the liquid film, and investigated the correlation between the meniscus around the particle and the capillary force. Furthermore, the acceleration of liquid has been confirmed via study of the microscale liquid dynamics in pillar arrays with microstructures[6, 13, 14]. Namely, the acceleration of the liquid is realized after interaction with some particles (**Fig. 1**). In the absence of tiny obstacles, the droplet spreads smoothly on a substrate (**Fig. 1 (left)**). One cannot see any deformation of the droplet shape nor any acceleration/ deceleration in the spreading process. If there exist tiny particles on the smooth substrate, on the other hand, the speed of spreading is locally changed by the interaction between MCL and particle(s), and the propagation of MCL is vigorously enhanced (**Fig. 1 (right)**). The details of those mechanisms, however, have been unclear.

Through this work we focus on the interaction between a single spherical particle and a liquid film spreading on a substrate, and the acceleration of the MCL after their interaction is investigated experimentally. Variation of the MCL velocity before and after the interaction between the particle and liquid is illustrated. Furthermore, the particle behavior after interaction with the liquid film is considered closely.

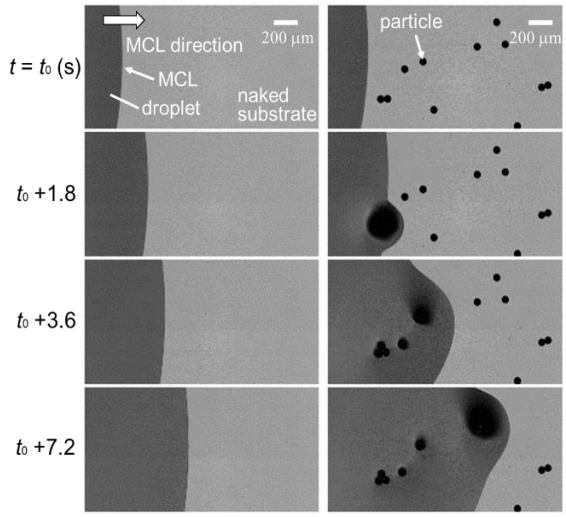

Fig. 1 Temporal evolution of the macroscopic contact line (MCL) of a droplet spreading on a smooth substrate observed from above; (left) naked substrate and (right) with randomly dispersed particles.

2. Experimental Setup

The experimental apparatus is shown in **Fig. 2**. Silicone oils of different viscosities (polydimethylsiloxane, KF-96L-2cs and KF-96L-6cs from Shin-Etsu Chemical Co., Ltd.) were used as the test fluids. Their physical properties are listed in **Table 1**. A single droplet (volume: 2.40 ± 0.05 μL) was formed through a fine needle attached to the micro-syringe, and gently placed on the silicon-wafer substrate of surface composed of SiO_2. The outside of needle tip was processed with fluoride for the droplet not to stick to the needle tip. The distance between the tip of the needle and the substrate was set approximately 2.0 mm because the original radius of liquid droplet before putting on the substrate was of around 0.83 mm. A single particle was set on the substrate and the distance between the particle and the center of the droplet was changed from 2 mm to 4 mm in order to change the velocity of the MCL. Gold-nickel-alloy-coated acrylic particles of D = 30, 40, and 50 μm in diameter were employed as the test particles; whose densities were 1.49×10^3, 1.47×10^3 and 1.47×10^3 kg/m^3, respectively. The test particles were the same kinds of the particles employed for the on-orbit experiments in the Japanese Experiment Module 'Kibo' aboard the International Space Station[15, 16]; it was examined that the particles are well dispersed in the silicone oils and the properties are stable even in long-duration experiment.

The behaviors of the liquid were visualized in two different ways: laser interferometry (**Fig. 2(a)**) and direct optical observation from above (**Fig. 2(b)**) with a high-speed camera. The interferometry, which is based on the Brewster angle microscope[17], consisted of the laser, spatial filter, collimator, and polarizers. The incident angle of the laser to the substrate was fixed at 74° and the light was detected by the high-speed camera with a resolution of 1280×1024 pixels and a frame rate up to 250 frames per second (fps). Continuous laser of 532 nm in wavelength was employed as the light source. In the top-view setup, the same camera and lens were used to trace the movements of MCL and particle. The substrate was cleaned by using acetone and subsequently dried and then by a plasma cleaner (Harrick, PDC-32G) for a duration of 10 min in prior to each experimental run.

Table 1 Properties of test fluids at 25 °C

	density [kg/m^3]	kinematic viscosity [m^2/s]	surface tension [J/m^2]	refractive index [-]
2 cSt	8.73×10^2	2.0×10^{-6}	1.8×10^{-2}	1.38~1.39
6 cSt	9.22×10^2	6.0×10^{-6}	2.0×10^{-2}	1.38~1.39

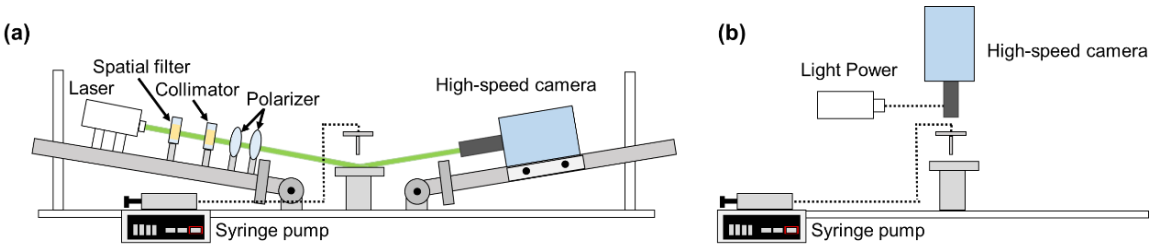

Fig. 2 Schematic of the experimental apparatus for (a) interferometry and (b) direct observation from above.

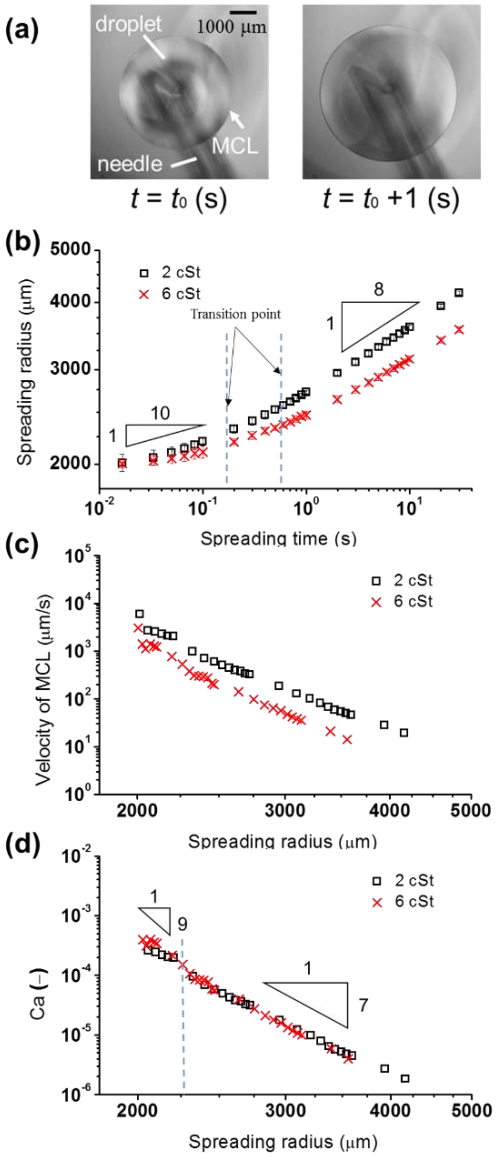

Fig. 3 Temporal variations of droplet radius and corresponding MCL velocity spreading on a smooth substrate without any particles; (a) typical example of the spreading process observed from above, (b) temporal variation of spreading radius, (c) variation of MCL velocity against spreading radius, and (d) variation of corresponding Ca against spreading radius.

3. Results & Discussion

Before discussing on the interaction between MCL and the particles on the smooth substrate, we indicate the characteristics of the behavior of the droplet spreading on a naked smooth substrate without any particle in order to validate our experimental systems.

Figure 3 shows typical examples of temporal variations of droplet radius and corresponding MCL velocity spreading on a smooth substrate without any particles. Panel (a) illustrates a typical example of the spreading process observed from above. We detect the position of MCL as a function of time from successive images monitored from above. Panel (b) indicates temporal variations of the droplet radius. Our droplet exhibits a change of the slope of the spreading radius against time; in the early stage the radius is proportional to $t^{1/10}$ following Tanner's law[8], and then to $t^{1/8}$ following Lopez law[7] after the gradual shift of the slope. Such tendency was also observed in the previous study[9]. We evaluate the corresponding velocity of MCL V_{CL} (panel (c)) from the temporal variation of the droplet radius, and further evaluate the corresponding capillary number Ca (panel (d)). We confirm that our droplets of different viscosities spreads by following Tanner's law[8] and then Lopez's law[7].

Figure 4 illustrates the dynamic contact angle versus capillary number. The contact angle is measured from the fringe patterns obtained in different experimental runs with the interferometry (**Fig. 2(a)**) under the same experimental conditions as shown in **Fig. 3**. We also confirm that our droplet spreads on a smooth substrate by exhibiting the contact angle $\propto$ $Ca^{1/3}$, which agrees well with the work of Hoffman[5].

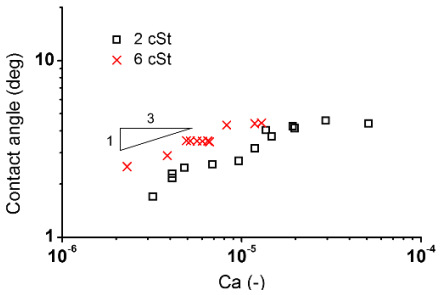

Fig. 4 Variation of contact angle against capillary number in the case without any particles.

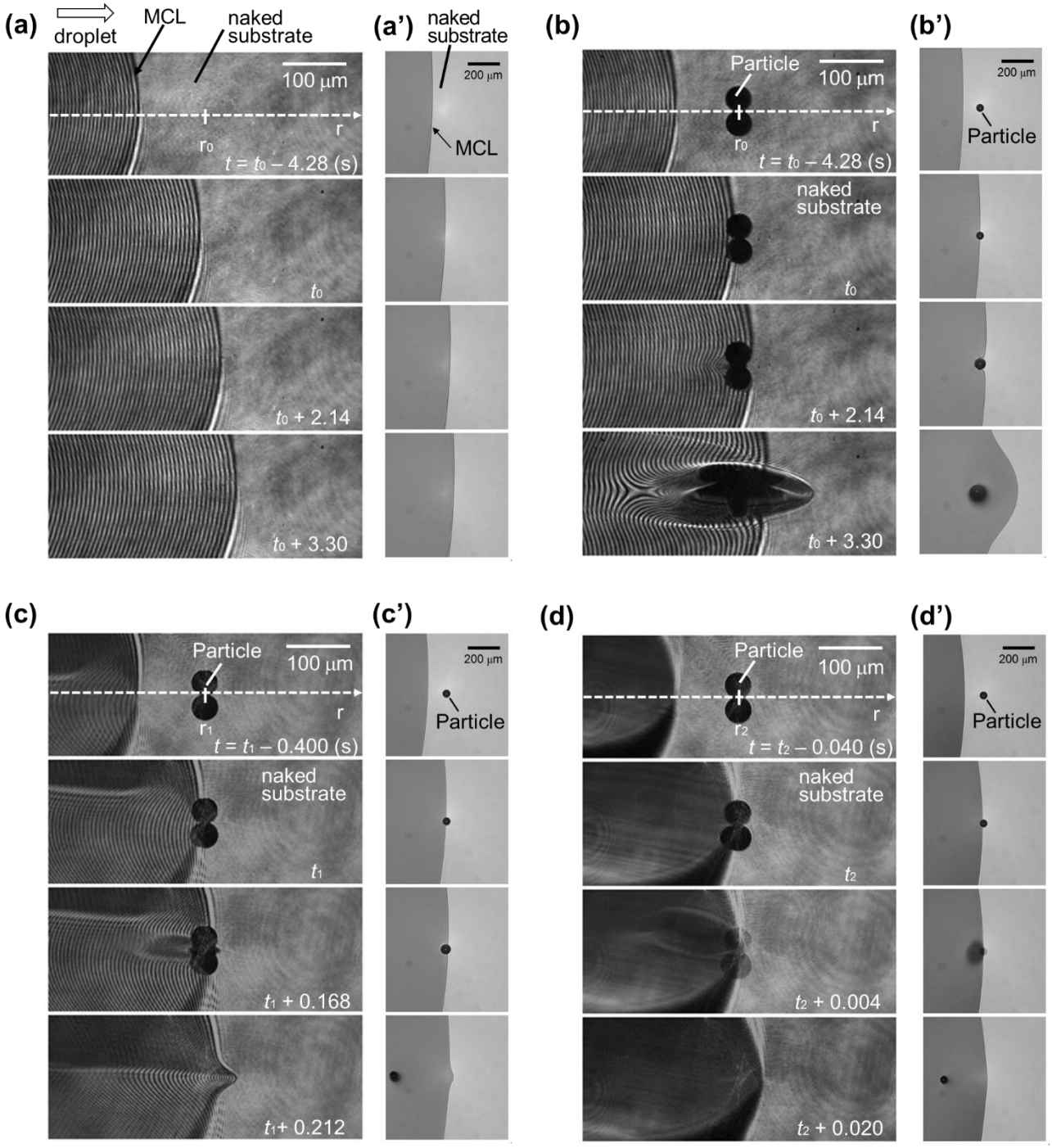

Fig. 5 Successive images of the MCL movement of droplet of the silicone oil of 2 cSt on a smooth substrate (a) without and (b)-(d) with a spherical particle of D = 40 μm settled ahead of the liquid film. Columns (a)-(d) indicate the fringe patterns obtained by the interferometry, and columns (a')-(d') indicate the top views. Conditions are (b) r_0 = 4 mm, Ca =1.40×10^{-6}, (c) r_1 = 3 mm, Ca = 9.07×10^{-6} and (d) r_2 = 2.4 mm, Ca =1.14×10^{-5}, where r_i indicates the distance between the centers of the droplet and the particle. The MCL spreads from left to right in all columns. The condition of (a) is the same as (b) but no particle on the substrate. Note that a mirror image of the particle is seen in (b)-(d) because of the inclined path of light against the substrate.

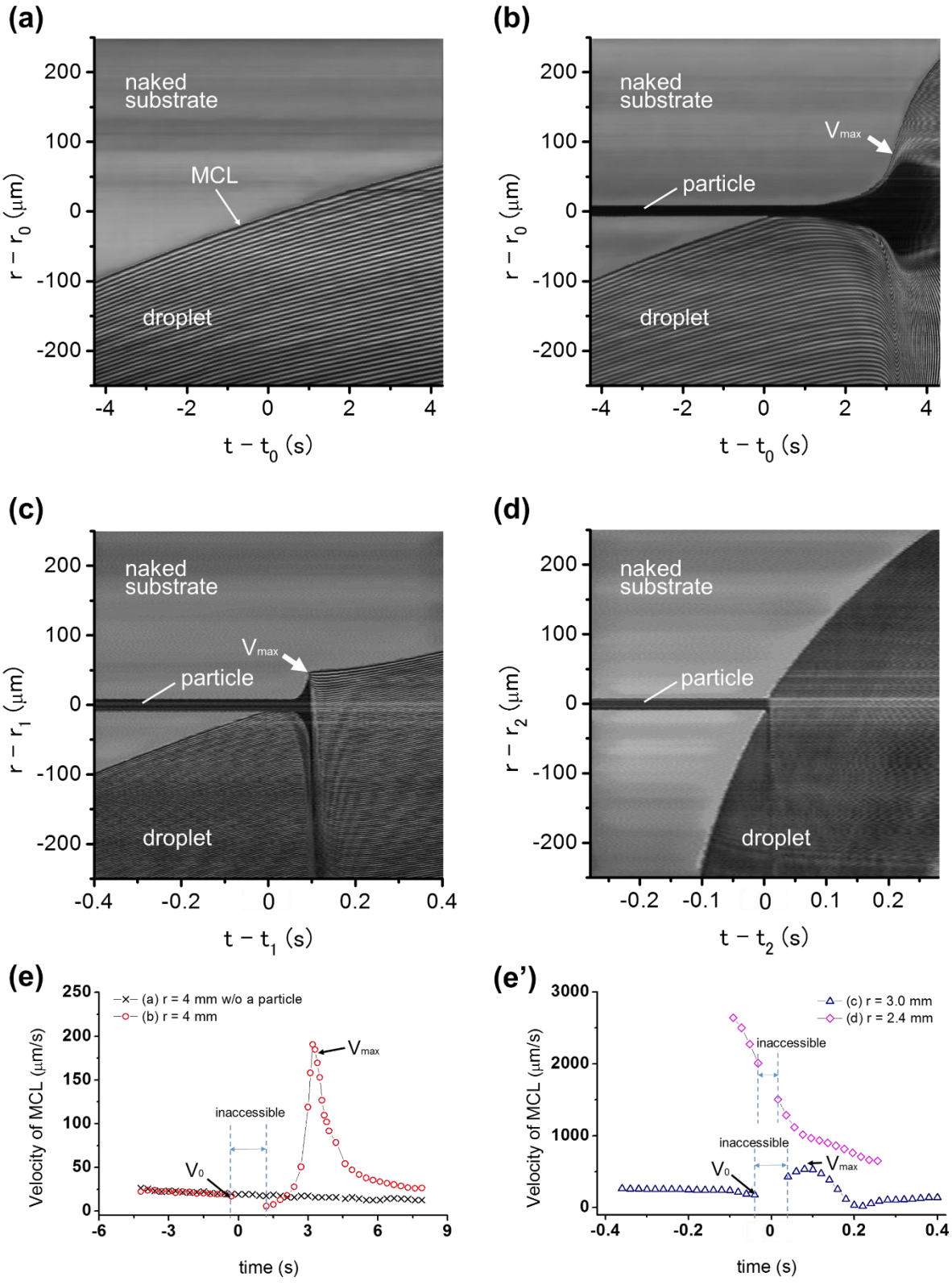

Fig. 6 (a)-(d) space-time diagrams constructed by arranging chronologically line images extracted from interferometry views along an axis passing both the droplet center and the particle foot. The diagram (a)-(d) correspond to the experiments in Fig. 5 (a)-(d), respectively. It should be noted the first fringe does not correspond to the MCL itself, but we confirm that the MCL lies very close to it according to our preliminary evaluation. Frame (e) and (e') illustrate the temporal variations of velocity of MCL reconstructed from fringe patterns as a function of time; frame (e) indicates the results of (a) and (b), and frame (e') the results of (c) and (d).

Figure 5 shows successive images of a droplet spreading on the substrate (a) without and (b)-(d) with a spherical particle of diameter 40 μm. Columns (a)-(d) indicate the fringe patterns obtained by the interferometry, and columns (a')-(d') indicate the top view images. By changing the distance, r_i, between the center of the droplet and the center of the particle on the substrate, the velocity of the MCL is varied. The characteristic velocity in Ca is defined as the velocity just prior to the interaction between the MCL and the particle foot. Corresponding conditions are (b) r_0 = 4 mm, Ca =1.40×10^{-6}, (c) r_1 = 3 mm, Ca = 9.07×10^{-6} and (d) r_2 = 2.4 mm, Ca =1.14×10^{-5}. In the case (a) without particle ahead the MCL on the substrate, the field of view is the same as shown in (b) but no particle on the substrate. In the case without particle (columns (a) and (a')), the MCL spreads as a function of time, and its velocity decreases as time elapses as described in **Figs. 3** and **4**. In the case of a single particle settled on the smooth substrate and smaller capillary number (10^{-6}) (in columns (b) and (b')), the MCL deforms after the interaction with the particle ($t = t_0$ + 2.14), and then sharp acceleration of the MCL is realized beyond the particle ($t = t_0$ + 3.30) as indicated by Mu et al.[18]. By decreasing r_i or increasing Ca (10^{-5}) (in columns (c) and (c')), the MCL follows a similar scenario to the case of (b) and (b'), but the deformation of MCL and its acceleration after the interaction become less. It is found that the particle is sucked toward the bulk of the droplet after the interaction with the MCL (see $t = t_1$ + 0.212 in (c')). Such a movement of the particle consumes the energy stored in the meniscus around the particle[18] to weaken the acceleration of MCL after the interaction. Further decreasing r_i or increasing Ca (10^{-4}), the MCL spreads on the substrate without any deformation and/or acceleration/deceleration even after the interaction with the particle (columns (d) and (d')), although the particle settled on the substrate is also sucked toward the bulk of the droplet as seen in the cases of (c) and (c').

Figures 6(a)-(d) illustrate the space-time diagram of the MCL along the line between the center of the droplet and the particle as shown in dashed line in **Figs. 5(a)-(d)**. One picks up the image as a thin band along the dashed line in the snapshot, and accumulated the bands obtained from successive images against time. The data as shown in **Figs. 6(a)-(d)** correspond to those shown in **Figs. 5(a)-(d)**. It should be noted that the edge of the fringes does not correspond to the MCL itself; one should reconstruct the droplet profile from fringe patterns in order to detect the precise position of the MCL. We confirm, however, that the MCL lies very close to the edge of the fringe patterns through the preliminary evaluation. Frame (e) and (e') illustrate the temporal variations of velocity of MCL reconstructed from fringe patterns as a function of time; frame (e) indicates the results of (a) and (b), and frame (e') the results of (c) and (d). Because of period during which the MCL very close to the particle is invisible, we do not plot any data but put 'inaccessible' in the diagrams. In the case without any particles on the substrate (a), the edge of the fringes or very close to the MCL travels with decreasing its velocity as time elapse, as aforementioned in **Fig. 5 (a)**. In the case of (b), it is clearly illustrated that the MCL exhibits a sharp acceleration after the interaction with a particle (horizontal black line in the diagram). It is found that the MCL velocity gradually decreases after reaching the maximum (arrow with 'V_{max}' in the frame). In the case of (c), the MCL exhibits a sharp acceleration after the interaction, but it abruptly decelerates. Such abrupt deceleration accompanies with the suck of the particle after the interaction with the MCL. In the case of (d) under larger Ca, the MCL never exhibits any variation in its propagation behavior even after the interaction with the particle; the temporal variation of the MCL position has a smooth profile as if no obstacle on the substrate.

Figures 7 shows the maximum MCL velocity (V_{max}) after the interaction with the particle in the case of the silicone oil as function of the capillary number. For these figures, the characteristic velocity is defined as the MCL velocity just prior to the interaction with a spherical particle as shown in **Figs. 6(e)** and **(e')**. **Figure 7(a)** shows the correlation between V_{max} and Ca; it is found that ln(V_{max}) increases linearly against ln(Ca) in region A. In this region, the particle remains stationary even after it interacts with the liquid film (i.e., $\Delta L/D \sim 0$, where ΔL indicates the displacement of the particle after the interaction with MCL). The correlation exhibits a transition from the region A to the region B ($\Delta L/D > 0$) as Ca increases. In the region B, ln(V_{max}) does not increase linearly against ln(Ca); the V_{max} scatters by changing Ca. In this region, we find that ΔL increases with Ca. The region C shows that ln(V_{max}) again increases linearly with ln(Ca); this reflects the situation of $V_{max} = V_0$ as aforementioned. In contrast to the region B, ΔL monotonically decreases as Ca increases in the region C. **Figure 7(b)** shows the correlation between V_{max}/V_0 and Ca for the particles of different sizes. The ratio V_{max}/V_0 is almost constant to be around 10 relative to Ca in the region A. V_{max}/V_0 starts decreasing as Ca increases throughout the region B. Finally, the maximum MCL velocity (V_{max}) matches the initial velocity (V_0) in the region C. The particle size D seems to have little effect on the results. **Figure 7(c)** shows the variations of the ratio V_{max}/V_0 against Ca when 2 cSt and 6 cSt silicone oils are used as the test fluid. It is indicated that the variation of V_{max}/V_0 almost matches despite of the liquid viscosity against Ca in a range of the particle sizes concerned. Such convergence concludes that the acceleration of the MCL after the interaction with a spherical particle is governed by the capillary number.

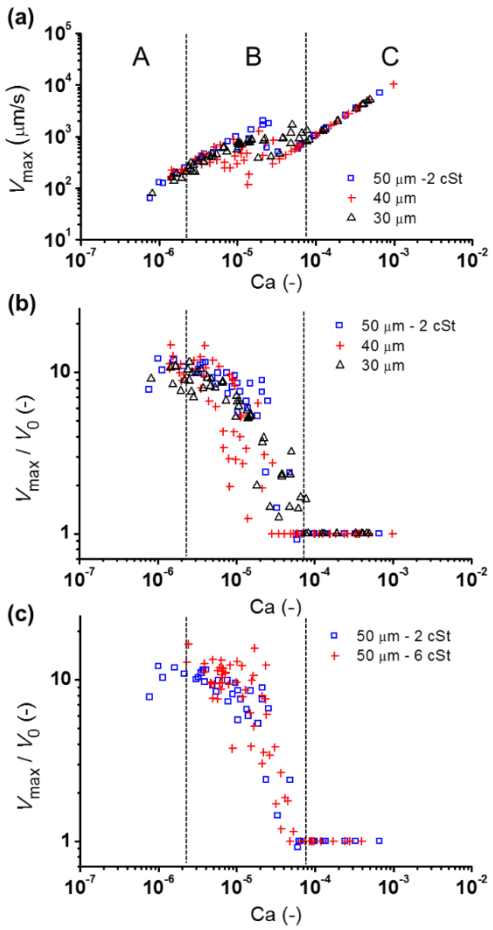

Fig. 7 (a) Maximum velocity of MCL, V_{max}, and (b)(c) maximum ratio of velocity variation, V_{max}/V_0 against capillary number, where V_0 is the MCL velocity just prior to interaction between MCL and particle. Frames (b) and (c) indicate variations of V_{max}/V_0 by changing the particle size in the case of droplet of 2 cSt and by changing droplet viscosity in the case of 50 μm diameter particle, respectively.

4. Concluding Remarks

We focus on the effect of the interaction with a spherical particle on the wetting behavior of thin liquid film spreading on a smooth substrate. Variation of the macroscopic contact line (MCL) of the droplet after the interaction is illustrated via the capillary number Ca. It is found that the acceleration of MCL occurs after the interaction between a liquid film and particle, depending on the capillary number Ca. The ratio of the maximum MCL velocity V_{max} to its initial velocity in just prior to the interaction with the particle V_0 is nearly independent of the capillary number in the case that the particle does not move even after the interaction. By increasing Ca, the particle exhibits a movement after the interaction with the MCL, then the ratio V_{max}/V_0 decreases as Ca, then no acceleration of MCL is realized even after the contact with the particle under Ca > 10^{-4}.

Acknowledgments

This work was partially supported by Grant-in-Aid for Challenging Exploratory Research from Japan Society for the Promotion of Science (JSPS) (grant number: 16K14176). IU acknowledges the support by Fund for Strategic Research Areas from Tokyo University of Science. International collaboration was supported by Bilateral Joint Research Projects 'SAKURA Program' by the Japan Society for the Promotion of Sciences (JSPS) and the Ministry of Foreign Affairs and International Development, France (MAEDI) for FY2015-2016. We gratefully acknowledge Prof. A. Komiya from Tohoku University, Japan, for his invaluable supports for setting up the experimental apparatus.

References

1) S. Ross and P. Becher: J. Colloid Interface Sci., **149** (1992) 575.
2) W. B. Hardy: Philos. Mag., **38** (1919) 49.
3) T. Young: Philos. T. R. Soci. Lond., **95** (1805) 65.
4) P. S. Laplace: Tome Premier [-quatrieme], **4** (1805).
5) R. L. Hoffman: J. Colloid Interface Sci., **50** (1975) 228.
6) J. Wang, M. Do-Quang, J.J. Cannon, F. Yue, Y. Suzuki, G. Amberg and J. Shiomi: Sci. Rep., **5** (2015) 8474.
7) J. Lopez, C. A. Miller and E. Ruckenstein: J. Colloid Interface Sci., **56** (1976) 460.
8) L. H. Tanner: J. Phys. D: Appl. Phys., **12** (1979) 1473.
9) A.-M. Cazabat and M.A. Cohen Stuart: J. Phys. Chem., **90** (1986) 5845.
10) P.A. Kralchevsky and K. Nagayama: Langmuir, **10** (1994) 23.
11) P.A. Kralchevsky and K. Nagayama: Adv. Colloid Interface Sci., **85** (2000) 145.
12) J. Ally, E. Vittorias, A. Amirfazli, M. Kappl, E. Bonaccurso, C.E McNamee and H.-J. Butt.: Langmuir, **26** (2010) 11797.
13) R. Xiao, R. Enright and E.N. Wang: Langmuir, **26** (2010) 15070.
14) R. Xiao and E. N. Wang: Langmuir, **27** (2011) 103.
15) T. Yano, K. Nishino, H. Kawamura, I. Ueno, S. Matsumoto, M. Ohnishi and S.I. Yoda: J. Jpn. Soc. Microgravity Appl, **28** (2011) S126.
16) T. Yano, K. Nishino, H. Kawamura, I. Ueno, S. Matsumoto, M. Ohnishi, and M. Sakurai: Experiments in fluids, **53** (2012) 9.
17) I. Ueno, K. Hirose, Y. Kizaki, Y. Kisara, and Y. Fukuhara: J. of Heat Transfer, **134** (2012) 051008.
18) L. Mu, D. Kondo, M. Inoue, T. Kaneko, H.N. Yoshikawa, F. Zoueshtiagh and I. Ueno: J. Fluid Mech, Rapids, **830** (2017) R1 .